

Short-Wavelength Infrared (SWIR) spectroscopy of low-grade metamorphic volcanic rocks of the Pilbara Craton



Mohammad S. Abweny^{a, b}, Frank J.A. van Ruitenbeek^{a, *}, Boudewijn de Smeth^a,
Tsehaie Woldai^c, Freek D. van der Meer^a, Thomas Cudahy^d, Tanja Zegers^e,
Jan-Kees Blom^f, Barbara Thuss^f

^a University of Twente, Faculty of Geo-Information Science and Earth Observation (ITC), Hengelosestraat 99, P.O. Box 37, Enschede 7500 AA, The Netherlands

^b Questerre Energy Corporation/Jordan (QEJ), Ibrahim Al-Qattan Street, Al-Rawabi County, Amman, Jordan

^c University of Witwatersrand, School of Geosciences, Private Bag X3, Wits 2050, Johannesburg, South Africa

^d CSIRO Earth Science and Resource Engineering, Minerals Down Under Flagship, 26 Dick Perry Avenue, Kensington WA 6151, Australia

^e Utrecht University, Faculty of Earth Sciences, Budapestlaan 17, 3584 CD Utrecht, The Netherlands

^f Delft University of Technology, Faculty of Civil Engineering and Geosciences, Stevinweg 1, 2628 CN Delft, The Netherlands

ARTICLE INFO

Article history:

Received 12 August 2013

Received in revised form

28 October 2015

Accepted 21 January 2016

Available online 22 January 2016

Keywords:

Infrared
Spectroscopy
Metamorphic
Volcanic
Archean
Mineralogy

ABSTRACT

This paper shows the results of Short-Wavelength Infrared (SWIR) spectroscopy investigations of volcanic rocks sampled from low-grade metamorphic greenstone belts of the Archean Pilbara Craton in Western Australia. From the reflectance spectra a range of spectrally active minerals were identified, including chlorites, hornblende, actinolite, epidote and white micas. The rock samples were grouped into mineral assemblages based on their spectrally identified minerals and stratigraphic positions. The metamorphic amphibolite and greenschist facies could be identified from the SWIR spectroscopic data as well as three sub zones of the greenschist facies: 1) a zone containing Fe-chlorite; 2) a zone containing intermediate chlorite and epidote; and 3) a zone containing intermediate chlorite, actinolite and hornblende. Spectral parameters were calculated from the reflectance spectra to assess the metamorphic grade and zones. Plots of the depth parameters of the Fe-OH feature near 2250 nm versus the Mg-OH feature near 2390 nm differentiate the metamorphic amphibolite and greenschist facies and a transition zone between the two. The wavelength position parameter of the Mg-OH absorption feature near 2340 nm also serves to discriminate between the various metamorphic sub zones.

The identification of the metamorphic grades of the volcanic sequences in greenstone belts with SWIR spectroscopy is useful for regional geological field studies, exploration for metamorphic mineral deposits hosted in the greenstone belts and the interpretation of hyperspectral remote sensing data sets covering similar types of terranes.

© 2016 Elsevier Ltd. All rights reserved.

1. Introduction

During metamorphism minerals contained in the rock recrystallize and new minerals may form, depending on the temperature and pressure and the chemical composition of the rock and the metamorphic fluids (Bucher and Grapes, 2011). Petrographic studies that include examination of the metamorphic mineralogy help to assess the metamorphic grade and reconstruct the pressure and temperature conditions that the rock has undergone.

Short-Wavelength InfraRed (SWIR) spectroscopy (between 1300 and 2500 nm) can be used to complement conventional petrographic studies on metamorphic rocks since the method allows for the detection of a range of indicative metamorphic minerals, including the phyllosilicates and inosilicates such as amphiboles (e.g., Clark et al., 1990). Studies of Duke (1994) and Duke and Lewis (2010) showed that variations in white micas detected with near-infrared spectroscopy in metasedimentary rocks enabled the mapping of metamorphic grade, ranging from very low grade to upper amphibolite facies. Longhi et al. (2000) established relationships between metamorphic grade and near-infrared spectra of siliceous muscovite-bearing rocks. Doublier et al. (2010a; 2012) demonstrated the usefulness of near-infrared spectroscopy of

* Corresponding author.

E-mail address: f.j.a.vanruitenbeek@utwente.nl (F.J.A. van Ruitenbeek).

chlorites to determine very low metamorphic grades in pelites. Bowen et al. (2007) used reflectance spectra of iron oxides, clays and carbonates to determined relationships between spatial heterogeneities in diagenetic mineralogy and paleofluid-migration pathways in Jurassic sandstones.

Systematic studies of SWIR spectroscopy of low-grade metamorphic volcanic rocks in greenstone belts, however, are limited. Most SWIR spectroscopy studies of volcanic rock in the literature focus on the identification of hydrothermal alteration minerals that are related to mineral deposits (e.g., Herrmann et al., 2001; Sun et al., 2001; Van Ruitenbeek et al., 2012). Wickert et al. (2008) studied reflectance spectra of mafic and ultramafic lithologies but focused on the effects of weathering on the spectral response.

The relatively low-pressure metamorphism of greenstone rocks is comparable to seafloor metamorphism in which rocks undergo low-grade metamorphism between 300° and 500 °C at low to intermediate pressure (Frey and Robinson, 1999). Minerals that are typical for greenschist or greenstone facies are Fe and Mg chlorites, the amphiboles hornblende and actinolite, epidote, sericite, albite and quartz. Transition of greenschist into higher grade amphibolite facies (>450 °C) is marked by predominance of hornblende (Bucher and Grapes, 2011). Metamorphic sub zones that result from changes in composition of the parent material and metamorphic conditions can be discriminated by their typical mineral assemblages (Terabayashi et al., 2003). Most of these metamorphic minerals have diagnostic features in the near-infrared wavelength region and can be detected with SWIR spectroscopy, except albite and quartz (Clark, 1999). Therefore, SWIR spectroscopy provides a tool to assess metamorphic grade and identify metamorphic sub zones.

This study presents the results of a systematic investigation of SWIR reflectance spectra of rock samples from greenstone sequences in the Archean Pilbara Craton in Northwest Australia (Thuss, 2005; Smithies et al., 2007) (Fig. 1). The volcanic rocks are predominantly of intermediate to mafic composition and have undergone low-grade metamorphism. The identification of the metamorphic grades of the volcanic sequences within greenstone belts with SWIR spectroscopy may be useful for regional geological

field studies, exploration for metamorphic mineral deposits hosted in the greenstone belts and the interpretation of hyperspectral remote sensing data sets covering similar types of terranes. Results also provide useful reference data for the interpretation of planetary data sets from areas where hydrated ferro-magnesian silicates have been identified (Ehlmann et al., 2009; Carter et al., 2013).

1.1. SWIR spectral mineralogy

Reflectance spectra of a range of metamorphic minerals that commonly occur in low-grade metamorphic rocks contain diagnostic absorption features between 1300 and 2500 nm. These features are related to absorption of infrared radiation by molecular bonds, such as bonds within Al-OH, Fe-OH, Mg-OH, OH and H₂O (Clark et al., 1990). SWIR reflectance spectra of selected metamorphic minerals and diagnostic absorption features are discussed in the following sub sections.

1.1.1. Chlorite

Chlorites are a group of phyllosilicate minerals containing Al, Mg and Fe end members. Their SWIR reflectance spectra show sharp absorption features near 1400 nm, 2250 nm and 2350 nm (Fig. 2) related to OH overtones, AlFe-OH or AlMg-OH combination bands and Mg₃-OH combination bands, respectively (Bishop et al., 2008; Doublier et al., 2012). The 2250 nm feature will subsequently be referred to as the Fe-OH absorption feature and the 2350 nm feature as the Mg-OH absorption feature of chlorite.

Spectrally, Mg and Fe varieties (as a result of Fe and Mg substitution) of chlorites can be identified using their Mg-OH and Fe-OH absorption features. The spectral positions of the Mg-OH and Fe-OH features depend mainly on the ratio of Fe/(Fe + Mg); both absorption bands shift to longer wavelength with increased Fe/(Fe + Mg) (McLeod et al., 1987; Merry et al., 1999). The main diagnostic spectral positions of the Mg-OH and Fe-OH absorption features are 2325 nm and 2245 nm for Mg-chlorite, respectively; and 2355 nm and 2261 nm for Fe-chlorite, respectively (Fig. 2). Chlorites of intermediate composition, e.g. intermediate chlorites, have Mg-OH and Fe-OH absorption features close to 2347 nm and

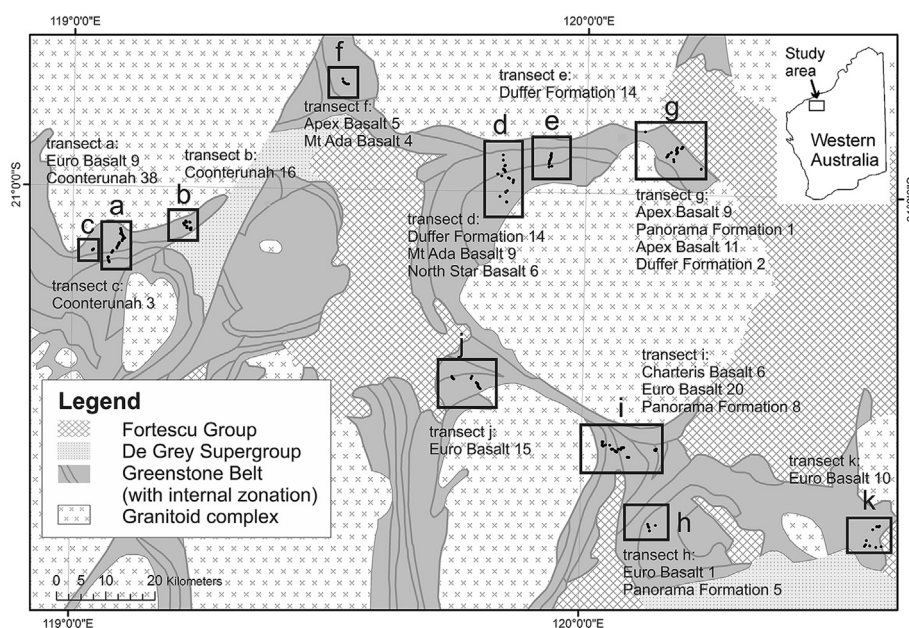


Fig. 1. Generalized geological map of the East Pilbara Granite-Greenstone Terrane in Western Australia showing locations of transects, rocks samples and number of samples collected from each of the stratigraphic units by Smithies et al. (2007).

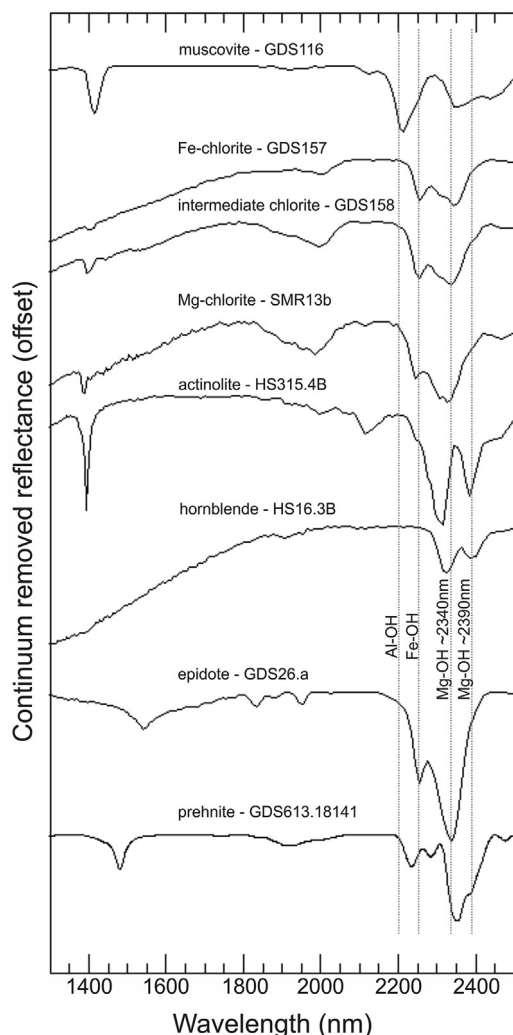


Fig. 2. Typical reflectance spectra of metamorphic minerals encountered in volcanic rocks in the study area. Vertical lines indicate wavelength position of the various spectral parameters that were discussed in this paper (Table 1). Spectra were obtained from the USGS spectral library (Clark et al., 2007).

2254 nm, respectively. In submarine environments, basaltic glass transforms to hydrated alteration products, i.e. palagonite, but at higher metamorphic grades it recrystallizes into silicates such as chlorite and smectite (Inoue and Utada, 1991). The ratio of Fe/(Fe + Mg) decreases with the increase in metamorphic grade and intensity of hydrothermal alteration (Shikazono and Kawahata, 1987; Frey and Robinson, 1999). As a consequence, Fe-rich chlorite tends to be stable in low temperature conditions and increases in distal parts of mineralized hydrothermal. In hydrothermal ore zones, coexisting minerals may affect the composition of chlorites. McLeod et al. (1987) found that lead-zinc ores are accompanied by lower ratios of Fe/(Fe + Mg) than copper-rich mineralization and interbedded volcanic and sedimentary rocks. In sub-greenschist and greenschist facies the average temperatures of formation of chlorite are approximately 260 °C and 310 °C respectively (Frey and Robinson, 1999).

1.1.2. Amphibole

Actinolite is a ferromagnesian mineral of the amphibole group. It is common in upper greenschist facies metamorphic rocks. It is an intermediate variety between magnesium-rich tremolite and iron-rich ferro-actinolite. Spectrally, two Mg-OH absorption features are

the main diagnostic features of actinolite and they vary between approximately 2314–2324 nm and 2380–2390 nm (Fig. 2) (Clark et al., 1990). Hornblende is another ferromagnesian mineral of the amphibole group that can be found in a wide variety of igneous rocks. In metamorphic rocks, it is common in transitional greenschist to amphibolite and amphibolite facies. Spectrally it has two main diagnostic absorption features related to Mg-OH between approximately 2324–2350 nm and between 2390 and 2410 nm (Fig. 2) (Clark et al., 2007).

To make a distinction between the two types of amphiboles with SWIR spectroscopy is complicated by the dependency of the wavelength positions of the Mg-OH absorption features on their chemical composition (Mustard, 1992; Laukamp et al., 2012). Compositional variation may lead to overlapping wavelength positions of the Mg-OH features between the two types of amphiboles. The compositional variation is difficult to recognize if other Mg-OH bearing minerals are present in the same rocks.

1.1.3. Epidote

The epidote group of minerals consists of Ca–Al–Fe³⁺ silicate minerals that are common in altered mafic to intermediate igneous rocks. They result from hydrothermal and metamorphic processes and form after various minerals, including feldspars, amphiboles, pyroxenes and micas. The iron to aluminum ratio (due to Fe³⁺–Al exchange) in epidote depends on the bulk rock composition and the pressure-temperature-fluid-redox conditions resulting in different minerals of the epidote group. In metabasites epidote tends to be more Fe-rich whilst in metapelites epidote contains less Fe (and more Al). Fe-rich epidote also indicates lower metamorphic grades (Grapes and Hoskin, 2004). The main spectral features are caused by Fe–OH absorptions and located at nearly 2255 nm and 2335–2342 nm, respectively (Fig. 2) (Clark et al., 1990). Other typical absorption features related to OH-bonds occur at 1540 nm and 1835 nm. The main absorption features overlap the absorption features of chlorite which may complicate the interpretation of mixed spectra of epidote and chlorite (Dalton et al., 2004).

1.1.4. Prehnite

Prehnite is a non-magmatic Ca–Al phyllosilicate mineral usually found in mafic volcanic and very low-grade metamorphic rocks. The mineral forms by secondary processes. It is considered as an indicator of very low-grade prehnite-pumpellyite metamorphic facies. The main spectral absorption features are near 1476 nm and 2350 nm (Fig. 2), the latter overlaps with the absorption features of other low-grade metamorphic minerals. Additionally, prehnite has weaker but distinctive features at 2230 nm and 2282 nm. Prehnite typically coexists with pumpellyite (another Ca–Al phyllosilicate) (Yuasa et al., 1992).

1.1.5. White mica

White micas are a group of phyllosilicates minerals including illite, paragonite, muscovite and phengite (Fleet et al., 2003). Sericite is fine-grained white mica. White micas are found in a wide variety of rocks, i.e. sedimentary, igneous and metamorphic, and environments due to weathering or alteration of feldspars (Guidotti, 1984; Velde and Meunier, 2008). Spectrally, white mica minerals are characterized by a prominent Al–OH absorption feature between approximately 2180 and 2235 nm (Doublier et al., 2010a) and two secondary diagnostic Al–OH absorption features close to 2344 nm and 2440 nm (Fig. 2) (Clark et al., 1990). Compositional variation of white micas can be observed by the wavelength position of the main Al–OH absorption feature that changes gradually from <2195 nm for paragonite as well as Al-rich white mica (Doublier et al., 2010b) to about 2200 nm in muscovite and up to 2235 nm in phengite (Doublier et al., 2010a).

except in the lower part adjacent to the granite intrusion, where it is metamorphosed to lower amphibolite facies.

1.2.3. Mount Ada Basalt Formation

The Mount Ada Basalt Formation (3469 ± 3 Ma) (Fig. 3) consists of an approximately 2.5 km thick sequence of mainly pillowed and massive basalt and komatiitic basalt with spinifex texture, felsic and mafic metavolcaniclastics and chert rocks. The formation conformably overlies either the McPhee Formation or the Dresser Formation in different greenstone belts and is conformably overlain by felsic volcanic rocks of the Duffer Formation. Weakly metamorphosed basalts at greenschist facies are pillowed and contain interpillow hyaloclastite. The komatiitic basalt unit is weakly metamorphosed at greenschist facies. Upper parts are marked by mafic with lesser felsic volcaniclastics, intercalated with milky gray chert.

1.2.4. Duffer Formation

The Duffer Formation (3474–3463 Ma) (Fig. 3), which is up to 4.75 km thick and consists predominantly of metamorphosed volcaniclastics and flows of dacitic to rhyolitic composition, especially in the lower half of the formation, in addition to pillowed tholeiitic basalt and layered sedimentary metachert. The formation conformably overlies the Mount Ada Basalt Formation and is unconformably overlain by the younger formations. Pillowed andesitic–basaltic rocks are metamorphosed at greenschist facies.

1.2.5. Apex Basalt Formation

The Apex Basalt Formation (3458–3410 Ma) (Fig. 3) forms the lower part of the Salgash Subgroup and is about 2.5 km thick. It unconformably overlies the Duffer Formation and is conformably overlain by the Panorama or Euro Basalt Formation. The rocks commonly contain actinolite–plagioclase–quartz assemblages with minor chlorite and epidote, and become darker with schistose amphibole–plagioclase assemblage at the contact with granitoid complexes.

1.2.6. Panorama Formation

The Panorama Formation (3456 Ma) (Fig. 3) is about 2 km thick. The formation structurally overlies the Apex Basalt and is overlain by the Strelley Pool Chert or unconformably by the Euro Basalt. The formation consists of a succession of metamorphosed felsic volcaniclastic rocks with agglomerate, silicified tuffaceous volcaniclastic rocks and minor volcanic breccia. At the top of the formation, the tuffaceous unit is crosscut by hydrothermal veins of black chert which are thought to be feeders for the overlying Strelley Pool Chert. The rocks of the felsic unit are altered, siliceous, porphyritic and fine-grained rhyolite to dacite and tuffaceous rocks. In the McFee greenstone belt, the formation consists of 3433–3426 Ma felsic volcaniclastic rocks with subordinate felsic lava and chert, and interbedded with andesitic basalt.

1.2.7. Euro Basalt Formation

The Euro Basalt Formation (3350–3325 Ma) (Fig. 3) conformably overlies the Strelley Pool Chert or unconformably overlies the Panorama Formation. It is structurally overlain by the Duffer, Apex and Charteris formations. In places, the Gorge Creek and Fortescue Groups unconformably overlie the formation. The formation consists of an approximately 9.4 km thick sequence of predominantly pillowed basalt and interbedded tholeiitic units and high Mg–basalt in addition to basaltic komatiite and thin beds of chert intercalated with felsic volcaniclastics. At the base of the formation, the rocks consist of high-Mg komatiitic basalt.

1.2.8. Charteris Basalt Formation

The Charteris Basalt Formation of less than 2 km thickness is the youngest rock unit in this study (Fig. 3). It belongs to the Kelly Group but has not yet been dated. It conformably overlies the Wyman Formation (consisting of felsic volcanic rocks). The formation consists of metamorphosed tholeiitic basalt interlayered with thin dolerite and minor komatiitic basalt that contains chlorite after pyroxene.

2. Methods

SWIR reflectance spectra were acquired from 207 rock samples that were originally collected by Smithies et al. (2007). The rocks were sampled from volcanic units of various composition (Fig. 3). The samples were carefully collected from fresh unweathered rocks without any visible veins or signs of alterations (Smithies et al., 2007). Petrographic analysis of thin sections, lithogeochemical data and geological maps and reports were applied to provide geological context to the rock samples and to compare, evaluate and validate interpretations of the reflectance spectra.

2.1. Reflectance spectroscopy

Reflectance spectra were obtained from each rock sample using an Analytical Spectral Devices FieldSpec Pro spectrometer within the range of 350–2500 nm. The spectral resolution of the instrument varied between 3 nm at 700 nm to 10 nm at longer wavelengths. From each sample three reflectance spectra were obtained for assessment of representativeness of the spectra. The ASD spectral files were splice corrected using the ViewSpecPro software and then converted to ASCII format. The spectra were first matched to library spectra using the Spectral Geologist software (Merry et al., 1999). Subsequently, each individual reflectance spectrum was visually interpreted by matching it with library spectra from the USGS (Clark et al., 2007) (Fig. 2). For each reflectance spectrum a maximum of three minerals could be interpreted. Interpretation of more than three minerals from a single spectrum did not give reliable results because of overlapping features between spectrally active minerals. The rock samples were grouped into metamorphic mineral assemblages based on i) the interpreted minerals they contained and ii) their stratigraphic positions within the greenstone belts.

Spectral parameters were calculated from the reflectance spectra to investigate the relationship between, on the one hand, the wavelength position and depth of specific absorption features and, on the other hand, the metamorphic mineral assemblage and metamorphic grade. The transition between assemblages was accompanied by i) the disappearance of some minerals and appearance of new minerals and ii) from the gradual change in composition of individual minerals, such as the Fe/(Fe + Mg) ratio of chlorite. Since these processes are gradual they can be monitored by the analysis of the spectral absorption features that respond to these gradual changes. The spectral parameters that were used in this study are listed in Table 1. The approximate wavelength positions of the calculated parameters are shown in Fig. 2.

Table 1
Spectral parameters calculated from the reflectance spectra.

Absorption feature	Wavelength range	Depth	Wavelength position
Al-OH ~ 2200 nm	2180–2228 nm		X
Fe-OH ~ 2250 nm	2238–2262 nm	X	
Mg-OH ~ 2340 nm	2310–2360 nm		X
Mg-OH ~ 2390 nm	2382–2404 nm	X	

2.2. Whole rock geochemistry

Whole rock geochemical data from Smithies et al. (2007) were used to relate the spectral data to the lithological composition of the volcanic rock and to verify that the chemical composition of the rocks had not been significantly modified by metasomatic and hydrothermal processes. Smithies et al. (2007) provided details of the geochemical data acquisition. XRF spectrometry was used to analyze major elements on fused disks similar to the methods of Norrish and Hutton (1969) with $\pm 1\%$ precision. LOI and Fe abundances were determined by gravimetry (after combustion at 1100 °C by digestion) and electrochemical titration using a modified methodology based on Shapiro and Brannock (1962).

The major element geochemical data set was checked prior to interpretation of lithology and estimation of intensity of hydrothermal alteration. Internal correlation problems of the major oxides were handled by application of the centered log-ratio transformation method (Filzmoser et al., 2010). The results showed no significant differences before and after applying the centered log-ratio transformation, therefore the original major elements data were used in this study. The major elements were converted to mole proportion for further use. The correlation between the major oxides was calculated in order to develop an empirically derived lithological index, where positively correlating oxides formed the numerator and negatively correlated major oxides formed the denominator.

3. Results and discussion

3.1. Metamorphic spectral minerals

Results of the spectral analysis showed that chlorite species,

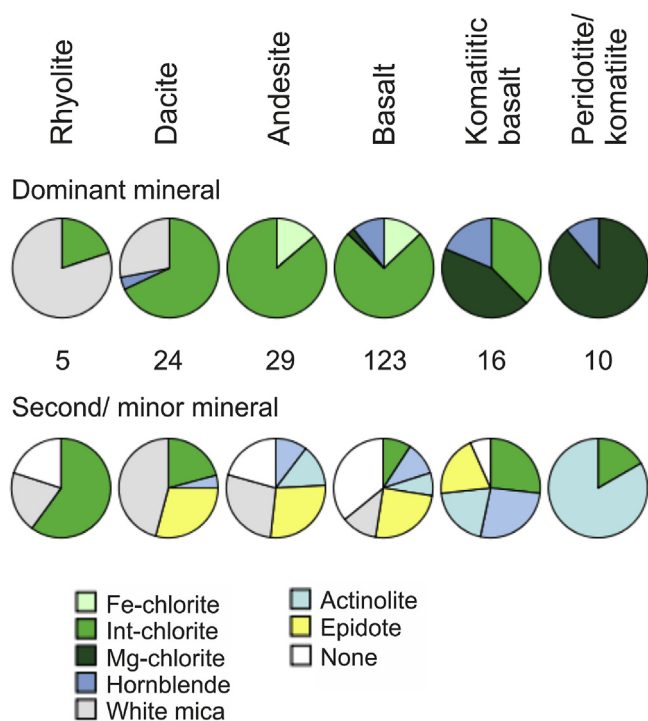


Fig. 4. Spectral minerals identified in the 207 rock samples in the different volcanic lithologies. The upper row shows the proportion of minerals of the dominant spectral minerals, the lower row shows the second or minor minerals in the various groups of rocks. "None" means that no second mineral was present in the spectrum. Minerals present in less than 5% of the rock samples were left out of the charts.

epidote, hornblende, actinolite and white micas were the main spectrally identifiable minerals in the volcanic rock samples (Fig. 4). Prehnite was found in only a few samples. Some minerals that were identified by thin section analysis could not be detected with SWIR spectroscopy, such as carbonates (calcite), quartz and feldspars. Detection of carbonates may not have been possible through the obscuring of their diagnostic absorption features by other minerals such as chlorites (Dalton et al., 2004).

Chlorites were the dominant spectral minerals. They were the dominant mineral in all lithological compositions, except in rhyolites where white micas were more dominant. The spectra of chlorites in the felsic and mafic rocks were consistent with predominantly intermediate Fe/(Fe + Mg) ratios and became more Mg rich in the komatiitic basalts, komatiites and peridotites (Fig. 4). Hornblende was more evident in mafic/ultramafic rocks compared with other lithologies. In most of the samples the minerals actinolite and epidote did not occur as the dominant spectral species, but as minor spectral minerals.

3.2. Spectral mixtures

Spectral mixing of metamorphic minerals posed problems with the manual interpretation of some of the spectra, especially in mixtures of minerals with overlapping features. The amphiboles actinolite and hornblende contained overlapping features and were difficult to distinguish. The discrimination of actinolite was based on a deeper main Mg-OH absorption feature close to 2315 nm, a shallower secondary Mg-OH absorption feature close to 2385 nm, and narrower and deeper absorption features close to 1400 nm and 1100 nm related to H₂O/OH (Fig. 2). The discrimination was also based on the shorter wavelength position of the Mg-OH absorption feature of actinolite relative to that of hornblende. Although spectral interpretations were confirmed by the results of petrographic analysis of selected samples, the discrimination between actinolite and hornblende in many samples remained uncertain.

Actinolite was often mixed with other minerals, such as chlorite. This caused overprinting of the main absorption feature of actinolite by absorption features of chlorite. In such mixtures, the examination of the secondary absorption features near 1400 and 1100 nm were used for the identification of actinolite and the differentiation from hornblende. The identification of epidote didn't pose problems since it contained unique secondary absorption features near 1540 nm and 1835 nm (Figs. 2 and 5B).

In mixed spectra of a dominant mineral with a second mineral present in minor quantities, the reflectance spectrum of the dominant mineral was modified by minor absorption features and inflexion points of the second mineral. Examples were spectral mixtures of chlorite with minor hornblende that contained a shallow absorption feature or inflexion around 2390 nm caused by the main Mg-OH absorption feature of hornblende (Fig. 5A). Spectra of dominant hornblende mixed with minor chlorite contained a shallow absorption feature or inflexion point around 2250 nm caused by the Fe-OH feature of chlorite.

3.3. Metamorphic grade

Fig. 6 shows the results of grouping the rock samples into spectrally determined mineral assemblages (column "Mineral assemblage") in relation to their stratigraphic position. Two main metamorphic facies, i.e. greenschist and amphibolite facies, were identified from the spectral mineralogical analysis (Fig. 7). Subdivisions could be made to the greenschist facies based on the presence of epidote, actinolite and hornblende in the spectral mineral assemblages. The transition from assemblages with epidote through assemblages containing actinolite to those with

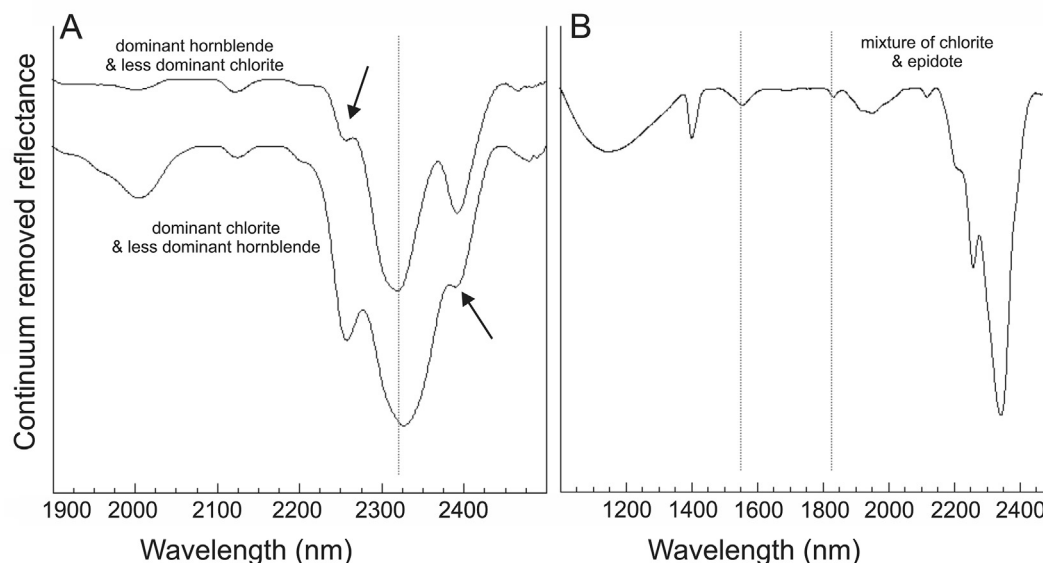


Fig. 5. Reflectance spectra of mixtures. (A) Spectral mixture of intermediate chlorite and hornblende. Arrows indicate shallow absorption features of the less abundant spectral mineral. The dotted line shows the position where both minerals overlap. (B) Spectral mixture of intermediate chlorite and epidote. Epidote can be identified using its shallow absorption features near 1540 nm and 1830 nm indicated by dotted lines.

hornblende indicated the increase in metamorphic grade within the greenschist facies whilst the appearance of hornblende as a dominant spectral mineral indicated the transition from greenschist to amphibolite facies (Fig. 7). Most of the spectral identifications of hornblende were found within the previously mapped amphibolite facies (Fig. 6, column "Metamorphic grade"). Occasionally, hornblende was also found in mafic–ultramafic rocks at higher stratigraphic positions of previously mapped lower metamorphic grade, which indicated the effect of lithology on the presence of hornblende. Chlorite minerals were found in both metamorphic facies where the transition from Fe rich to Mg rich chlorite indicated an increase in the metamorphic grade. The effect of changing mineralogy with metamorphic grade was enhanced by the presence of other indicator minerals such as epidote, actinolite and hornblende. The presence of Mg-chlorite was also affected by lithological composition. The mineral was found in ultramafic rocks and several high Mg-basalts, independent of their stratigraphic position and metamorphic grade. This suggests that the formation of Mg-chlorite is controlled by both metamorphic grade and lithological composition.

Local variations in spectral mineralogical assemblages (Fig. 6) were attributed to the texture and permeability of the volcanic rocks and local variations in the bulk lithological composition in addition to the metamorphic grade in terms of temperature, pressure and composition of fluids. The irregular distribution of prehnite, representing subgreenschist prehnite/pumpellyite metamorphic facies, was interpreted as the result of retrograde metamorphic processes.

3.4. Depth parameters of the Mg-OH and Fe-OH absorption features

Fields of similar metamorphic assemblages could be constructed in Fig. 8 by plotting of the two spectral depth parameters of the secondary Mg-OH (near 2390 nm) and main Fe-OH (near 2250 nm) absorption features (Table 1). Fig. 8A shows the fields that correspond to the two metamorphic greenschist and amphibolite facies which were constructed with data on metamorphic grade from the literature. Fig. 8B shows that the spectrally interpreted

hornblende was dominant in the amphibolite facies in the upper-left field while spectrally interpreted chlorite dominated in the greenschist facies field in the lower-right. Minor hornblende together with abundant chlorite marked the transition from greenschist to amphibolite facies (Fig. 8C). Some rocks containing Mg-chlorite also plotted in the field of the transition zone. Toward the amphibolite facies, hornblende became more dominant at the expense of chlorite, epidote and actinolite.

Within the greenschist facies, sub zones of i) abundant intermediate chlorite and less abundant epidote and ii) abundant intermediate chlorite and less abundant actinolite could be identified based on the presence/absence of epidote and actinolite (Fig. 8D). The transition from dominant chlorite (\pm epidote) through dominant chlorite and minor actinolite and hornblende to dominant hornblende was related to the transition from the metamorphic greenschist, through transition zone to amphibolite facies.

The depth parameters of SWIR spectra of minerals without Mg-OH features near 2390 nm or Fe-OH absorption features near 2250 nm were set to zero, indicating low or zero abundance. The depth of the Fe-OH absorption feature increased in response to increased spectral dominance of chlorite, whereas the depth of the secondary Mg-OH feature increased with increased spectral dominance of actinolite and hornblende. An advantage of using these depth parameters is their insensitiveness to the influence of sericite and carbonate minerals since the latter minerals don't contain absorption features in these wavelength ranges. Caution should be taken when calculating and plotting these parameters from samples that contain minerals with overlapping absorption features near 2390 nm other than those described in this study.

3.5. Wavelength position of Mg-OH absorption feature

For each of the mineral assemblages the wavelength position parameter of the Mg-OH feature was calculated (Table 1) since this parameter showed a good correlation with the metamorphic mineral assemblage (Fig. 6). Based on the wavelength position of the Mg-OH absorption feature near 2335 nm a division could be made into greenschist facies (2323–2356 nm), amphibolite facies

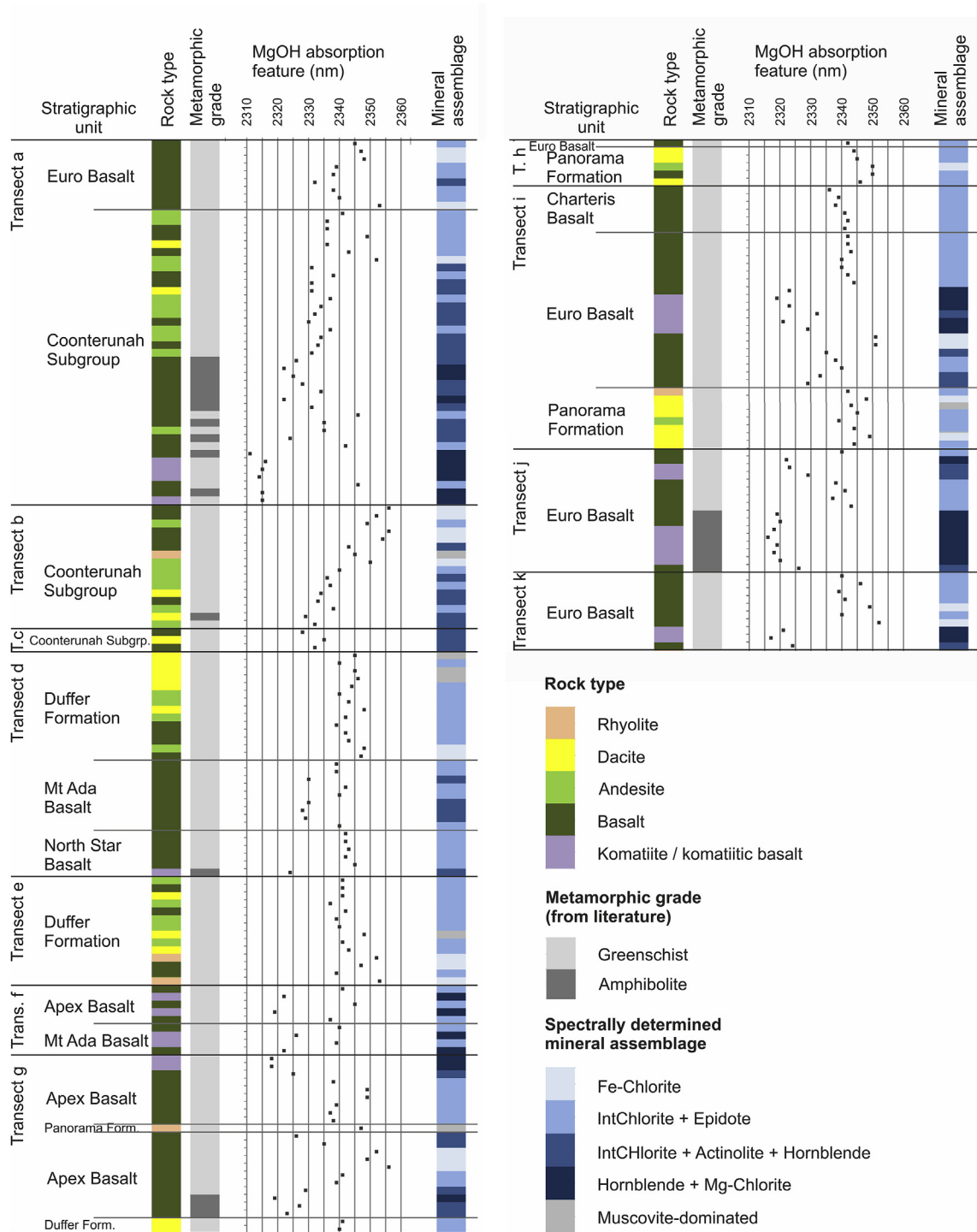


Fig. 6. Plot of the wavelength position of the Mg-OH absorption feature near 2340 nm (Table 1) of rocks collected along the transects in Fig. 1. Stratigraphic unit (Fig. 3), rock type (from Smithies et al. (2007)), metamorphic grade (from literature, see literature references in Section 1.2) and spectrally determined mineral assemblages are shown for each sample. Stratigraphic units in each transect are ordered from young (top) to bottom (old).

(2311–2329 nm) and a transition zone between the two (2323–2329 nm) (Fig. 7). The greenschist metamorphic facies could be further subdivided into three subzones (sub facies) from lower to higher grade: Fe-chlorite (2347–2356 nm), intermediate chlorite + epidote (2336–2347 nm) and intermediate chlorite + actinolite + hornblende (2324–2336 nm). The boundaries between different zones within the greenschist facies were sharp due to the abrupt change in mineralogy (appearance of new

spectral mineral(s) when changing to a different zone) whereas the boundary between the greenschist and amphibolite facies was more gradual due to the gradual increase of hornblende. The differentiation between Mg-chlorite and hornblende using the wavelength position parameter was not possible and therefore they fell in the same category of both the amphibolite facies and ultramafic lithological composition.

Fig. 9 shows the relationship between the lithological

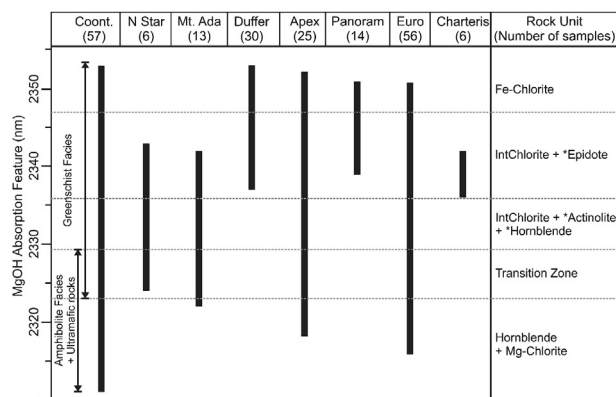


Fig. 7. Wavelength position of the Mg-OH absorption feature near 2340 nm of the rock samples grouped according to metamorphic mineral assemblage in the various stratigraphic formations (Fig. 3). Compiled literature data of the metamorphic grade of the rock samples is presented by the vertical arrows on the left of the figure. * = less abundant spectral mineral.

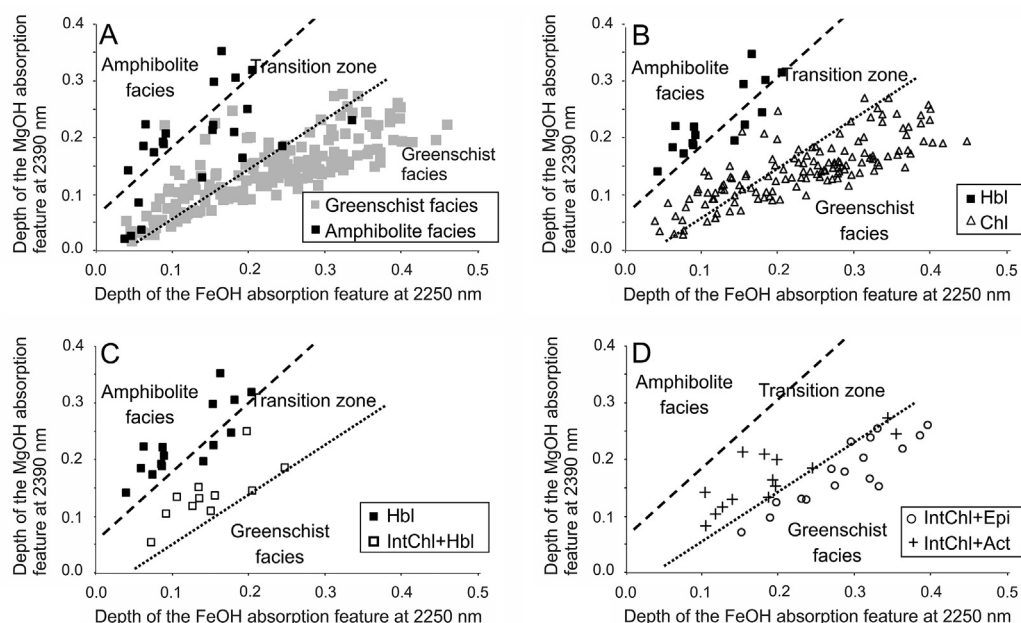


Fig. 8. Plots of depth parameters calculated from the reflectance spectra of rock samples. Fields of the metamorphic facies were interpreted from the data. A: Metamorphic grade of samples (data obtained from literature); B: Rock samples containing dominant hornblende and chlorite; C: Rock samples containing either dominant hornblende or dominant intermediate chlorite and secondary hornblende; D: Rock samples containing either intermediate chlorite and epidote or intermediate chlorite and actinolite. Hbl = hornblende; Chl = chlorite; IntChl = intermediate chlorite; Epi = epidote; Act = actinolite.

composition of the volcanic rocks and the spectral mineralogy, represented by the Mg-OH absorption feature. The spectral mineralogy reflects the effects of metamorphic grade rather than that of lithological composition, except for rhyolitic and ultramafic rocks. The influence of metamorphic grade was clear in the group of basaltic rocks with a relatively homogenous chemical composition and a large variation of spectral minerals.

4. Summary and conclusions

The study showed that the spectral characteristics of low-grade metamorphosed volcanic rocks were strongly influenced by the effects of metamorphic grade and to a lesser extent by the lithological composition of the rocks. The metamorphic facies that could

be spectrally identified are: 1) amphibolite facies, 2) a transition zone of amphibolite to greenschist facies, and 3) greenschist facies. The greenschist facies was subdivided into three sub zones: i) a Fe-chlorite zone, ii) an intermediate chlorite and epidote zone and iii) an intermediate chlorite, actinolite and hornblende zone. In previous studies with non-spectral methods, only the main metamorphic amphibolite and greenschist facies were described. In this study, boundaries between the greenschist subfacies were sharp due to appearance of new spectral minerals such as epidote and actinolite whereas the boundary between greenschist and amphibolite facies was transitional due to the gradual increase of hornblende.

The spectral position parameter of the Mg-OH absorption feature between 2310 and 2360 nm and the depth parameters of the secondary Fe-OH (near 2250 nm) and Mg-OH (near 2390 nm) absorption features were useful for characterizing the metamorphic grade of the different volcanic rock types. The three spectral parameters responded to the relative abundances of the metamorphic minerals, chlorite, actinolite, hornblende, epidote

and to the Fe/(Fe + Mg) ratio of chlorite. Prehnite-pumpellyite metamorphic facies, as well as the carbonate minerals, could not be detected using the main Mg-OH (2310–2360 nm) absorption feature because of overlap with other dominant Mg-OH and Fe-OH containing minerals. Basaltic rocks appeared to have the largest variety of spectral minerals and therefore are the best indicators of the metamorphic zones in this study. The spatial distribution of the mineral assemblages determined from the reflectance spectra is consistent with the position within the stratigraphic sequences, i.e. the metamorphic grade increased with depth in the volcanic sequence.

We conclude that SWIR spectroscopy can be applied to identify mineral assemblages and assess metamorphic grade in intermediate to mafic volcanic rocks typical for Archean greenstone belts.

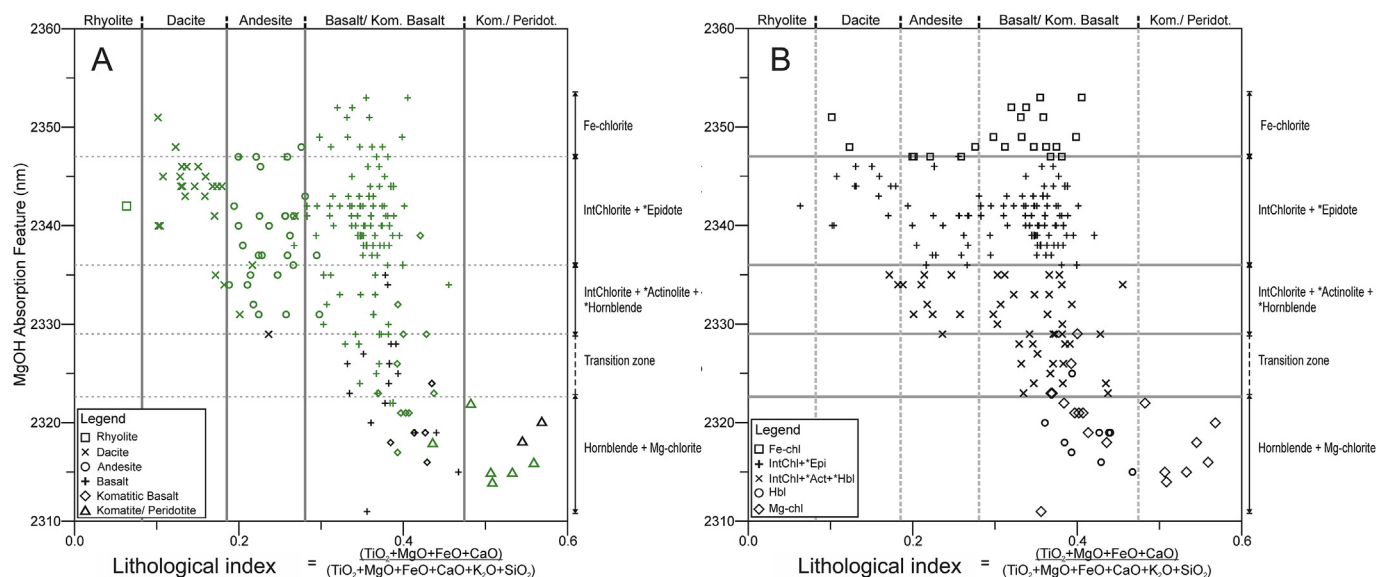


Fig. 9. Plots of the lithological index (Section 2.2) indicating lithological composition of the samples versus the wavelength position parameter of the Mg-OH absorption feature near 2340 nm. Spectrally determined mineral assemblages plotted along the Y-axis on the right. Samples containing dominant white mica were omitted from the figure. A: Symbols show the lithological composition information compiled from Smithies et al. (2007); colors indicate metamorphic grade obtained from literature (green = greenschist facies; black = amphibolite facies). B: Symbols represent mineral assemblages interpreted from the reflectance spectra. * = less abundant spectral mineral. (For interpretation of the references to colour in this figure legend, the reader is referred to the web version of this article.)

Abundances of metamorphic minerals, such as chlorites, amphiboles and epidote vary systematically within the greenstone sequences and their occurrences are associated with metamorphic grade, ranging from greenschist to amphibolite facies. Plots of spectral parameters, calculated from the reflectance spectra of volcanic rock samples, proved to be useful for the determination of the metamorphic facies and sub zones within the metamorphic facies. SWIR spectroscopy provides a field tool for assessing of metamorphic mapping in geological mapping studies. The results of this study provide a framework for the interpretation of hyperspectral remote sensing imagery of terrestrial and planetary studies in similar types of terranes.

Acknowledgments

We thank Hugh Smithies of the Geological Survey of Western Australia for making the rock samples available that were used in this study. This research was made possible by the financial support of the joint Japan/World Bank Graduate Scholarship Program (JJ/WBGSP). The field work activities were financially supported by the Foundation Stichting Dr. Schürmannfonds, grant no. 2002/22. We thank Edward Duke for his careful review that significantly improved the manuscript.

References

- Bagas, L., 2005. Geology of the Nullagine 1: 100 000 Sheet, 1: 100,000 Geological Series Explanatory Notes. Geological Survey of Western Australia, Perth, p. 33.
- Bishop, J.L., Lane, M.D., Dyar, M.D., Brown, A.J., 2008. Reflectance and emission spectroscopy study of four groups of phyllosilicates: smectites, kaolinite-serpentines, chlorites and micas. *Clay Miner.* 43, 35–54.
- Bowen, B.B., Martini, B.A., Chan, M.A., Parry, W.T., 2007. Reflectance spectroscopic mapping of diagenetic heterogeneities and fluid-flow pathways in the Jurassic Navajo Sandstone. *Aapg Bull.* 91, 173–190.
- Bucher, K., Grapes, R., 2011. *Metamorphic Grade, Petrogenesis of Metamorphic Rocks*. Springer, New York, pp. 119–187.
- Carter, J., Poulet, F., Murchie, S., Bibring, J.P., 2013. Automated processing of planetary hyperspectral datasets for the extraction of weak mineral signatures and applications to CRISM observations of hydrated silicates on Mars. *Planet. Space Sci.* 76, 53–67.
- Clark, R.N., 1999. Chapter 1: spectroscopy of rocks and minerals, and principles of

- spectroscopy. In: Rencz, A.N. (Ed.), *Manual of Remote Sensing*. John Wiley and Sons, New York, pp. 3–58.
- Clark, R.N., King, T.V.V., Klejwa, M., Swayze, G.A., Vergo, N., 1990. High spectral resolution reflectance spectroscopy of minerals. *J. Geophys. Res. Solid* 95, 12653–12680.
- Clark, R.N., Swayze, G.A., Wise, R., Livo, K.E., Hoefen, T.M., Kokaly, R.F., Sutley, S.J., 2007. USGS Digital Spectral Library Splib06a. Digital Data Series 231. U.S. Geological Survey, Denver.
- Dalton, J.B., Bove, D.J., Mladinich, C.S., Rockwell, B.W., 2004. Identification of spectrally similar materials using the USGS Tetracorder algorithm: the calcite-epidote-chlorite problem. *Remote Sens. Environ.* 89, 455–466.
- Doublier, M.P., Roache, A., Potel, S., 2010a. Application of SWIR Spectroscopy in Very Low-grade Metamorphic Environments: a Comparison with XRD Methods. *Geological Survey of Western Australia*, p. 61. Record 2010/7.
- Doublier, M.P., Roache, T., Potel, S., 2010b. Short-wavelength infrared spectroscopy: a new petrological tool in low-grade to very low-grade pelites. *Geology* 38, 1031–1034.
- Doublier, M.P., Roache, T., Potel, S., Laukamp, C., 2012. Short-wavelength infrared spectroscopy of chlorite can be used to determine very low metamorphic grades. *Eur. J. Mineral.* 24, 891–902.
- Duke, E.F., 1994. Near-infrared spectra of muscovite, Tschermak substitution, and metamorphic reaction progress - implications for remote sensing. *Geology* 22, 621–624.
- Duke, E.F., Lewis, R.S., 2010. Near infrared spectra of white mica in the Belt Supergroup and implications for metamorphism. *Am. Mineral.* 95, 908–920.
- Ehlmann, B.L., Mustard, J.F., Swayze, G.A., Clark, R.N., Bishop, J.L., Poulet, F., Marais, D.J.D., Roach, L.H., Milliken, R.E., Wray, J.J., Barnouin-Jha, O., Murchie, S.L., 2009. Identification of hydrated silicate minerals on Mars using MRO-CRISM: geologic context near Nili Fossae and implications for aqueous alteration. *J. Geophys. Res. Planets* 114, 1991–2012.
- Farrell, T., 2006. Geology of the Eastern Creek 1: 100 000 Sheet, 1: 100,000 Geological Series Explanatory Notes. Geological Survey of Western Australia, Perth, p. 33.
- Filzmoser, P., Hron, K., Reimann, C., 2010. The bivariate statistical analysis of environmental (compositional) data. *Sci. Total Environ.* 408, 4230–4238.
- Fleet, M.E., Deer, W.A., Howie, R.A., Zussman, J., 2003. *Rock-forming Minerals: Micas*, second ed. Geological Society of London, London.
- Frey, M., Robinson, D., 1999. *Low-grade Metamorphism*. Blackwell Science, Cambridge.
- Grapes, R.H., Hoskin, P.W.O., 2004. Epidote group minerals in low-medium pressure metamorphic terranes. *Rev. Mineral. Geochem.* 56, 301–345.
- Guidotti, C.V., 1984. Micas in metamorphic rocks. In: Bailey, S.W. (Ed.), *Micas*. Mineralogical Society of America, pp. 357–467.
- Herrmann, W., Blake, M., Doyle, M., Huston, D., Kamprad, J., Merry, N., Pontual, S., 2001. Short Wavelength InfraRed (SWIR) spectral analysis of hydrothermal alteration zones associated with base metal sulfide deposits at Rosebery and Western Tharsis, Tasmania, and Highway-Reward, Queensland. *Econ. Geol. Bull. Soc.* 96, 939–955.
- Hickman, A.H., 2004. Two contrasting granite-greenstone terranes in the Pilbara

- Craton, Australia: evidence for vertical and horizontal tectonic regimes prior to 2900 Ma. *Precambrian Res.* 131, 153–172.
- Inoue, A., Utada, M., 1991. Smectite-to-chlorite transformation in thermally metamorphosed volcanoclastic rocks in the Kamikita Area, Northern Honshu, Japan. *Am. Mineral.* 76, 628–640.
- Laukamp, C., Termin, K.A., Pejčić, B., Haest, M., Cudahy, T., 2012. Vibrational spectroscopy of calcic amphiboles – applications for exploration and mining. *Eur. J. Mineral.* 24, 863–878.
- Longhi, I., Mazzoli, C., Sgavetti, M., 2000. Determination of metamorphic grade in siliceous muscovite-bearing rocks in Madagascar using reflectance spectroscopy. *Terra Nova* 12, 21–27.
- McLeod, R.L., Gabell, A.R., Green, A.A., Gardavsky, V., 1987. Chlorite infrared spectral data as proximity indicators of volcanogenic massive sulphide mineralization. In: *Pacific Rim Congress, Gold Coast, Australia*, pp. 26–29.
- Merry, N., Pontual, S., Gamson, P., 1999. The Spectral Geologist “TSG” V. 2.0 User Manual. AusSpecInternational Pty. Ltd. Commonwealth Scientific and Industrial Research Organisation (CSIRO), Australia, p. 136.
- Mustard, J.F., 1992. Chemical-analysis of actinolite from reflectance spectra. *Am. Mineral.* 77, 345–358.
- Norrish, K., Hutton, J.T., 1969. An accurate X-ray spectrographic method for analysis of a wide range of geological samples. *Geochim. Cosmochim. Acta* 33, 431–453.
- Shapiro, L.M., Brannock, W.W., 1962. Rapid Analysis of Silicate, Carbonate and Phosphate Rocks. US Government Printing Office.
- Shikazono, N., Kawahata, H., 1987. Compositional differences in chlorite from hydrothermally altered rocks and hydrothermal ore-deposits. *Can. Mineral.* 25, 465–474.
- Smithies, R.H., Champion, D.C., Van Kranendonk, M.J., Hickman, A.H., 2007. Geochemistry of Volcanic Rocks of the Northern Pilbara Craton, Western Australia. Geological Survey of Western Australia, p. 47.
- Sun, Y.Y., Seccombe, P.K., Yang, K., 2001. Application of short-wave infrared spectroscopy to define alteration zones associated with the Elura zinc-lead-silver deposit, NSW, Australia. *J. Geochem. Explor.* 73, 11–26.
- Terabayashi, M., Masada, Y., Ozawa, H., 2003. Archean ocean-floor metamorphism in the North Pole area, Pilbara Craton, Western Australia. *Precambrian Res.* 127, 167–180.
- Thuss, B., 2005. Spectroscopic Study of Early Archean Volcanic Rocks in the Pilbara Craton (Western Australia). Technical University Delft (B.Sc. thesis).
- Van Kranendonk, M.J., 2000. Geology of the North Shaw 1: 100,000 Sheet, Western Australia, 1: 100,000 Geological Series Explanatory Notes. Geological Survey of Western Australia, Perth, p. 89.
- Van Kranendonk, M.J., 2010. Geology of the Coongan 1: 100,000 Sheet, Western Australia, 1: 100,000 Geological Series Explanatory Notes. Geological Survey of Western Australia, Perth, p. 67.
- Van Kranendonk, M.J., Hickman, A.H., Smithies, R.H., Williams, I.R., Bagas, L., Farrell, T.R., 2006. Revised Lithostratigraphy of Archean Supracrustal and Intrusive Rocks in the Northern Pilbara Craton, Western Australia. Western Australia Geological Survey, p. 57.
- Van Kranendonk, M.J., Smithies, R.H., Hickman, A.H., Champion, D., 2007. Review: secular tectonic evolution of Archean continental crust: interplay between horizontal and vertical processes in the formation of the Pilbara Craton, Australia. *Terra Nova* 19, 1–38.
- Van Ruitenbeek, F.J.A., Cudahy, T.J., van der Meer, F.D., Hale, M., 2012. Characterization of the hydrothermal systems associated with Archean VMS-mineralization at Panorama, Western Australia, using hyperspectral, geochemical and geothermometric data. *Ore Geol. Rev.* 45, 33–46.
- Velde, B.B., Meunier, A., 2008. The Origin of Clay Minerals in Soils and Weathered Rocks. Springer Science & Business Media, Berlin Heidelberg.
- Wickert, L.M., Percival, J.B., Morris, W., Harris, J.R., 2008. XRD and Infrared Spectroscopic Validation of Weathering Surfaces from Ultramafic and Mafic Lithologies Examined Using Hyperspectral Imagery, Cross Lake Area, Cape Smith Belt, Northern Quebec, Canada. Geoscience and Remote Sensing Symposium, 2008. IGARSS 2008. IEEE International. IEEE, Boston pp. III-362–III-365.
- Williams, I.R., 1999. Geology of the Muccan 1: 100 000 Sheet, 1: 100,000 Geological Series Explanatory Notes. Geological Survey of Western Australia, Perth, p. 39.
- Williams, I.R., Bagas, L., 2007. Geology of the Mount Edgar 1: 100 000 Sheet, 1:100 000 Geological Series Explanatory Notes, 1:100 000 Geological Series Explanatory Notes. Geological Survey of Western Australia, Perth, p. 62.
- Yuasa, M., Watanabe, T., Kuwajima, T., Hirama, T., Fujioka, K., 1992. Prehnite-pumpellyite facies metamorphism in oceanic arc basement from Site 791 in the Sumisu Rift, Western Pacific. In: *Proceedings of the Ocean Drilling Program, Scientific Results*, Houston, pp. 185–193.